

## Potential and Actual Predictability of Snow Water Equivalent in Historical Forecasts of the Canadian Fourth Generation Coupled Climate Model (CanCM4)

Reinel Sospedra-Alfonso and William J. Merryfield

*Canadian Centre for Climate Modelling and Analysis, University of Victoria, Canada*

### 1. Introduction

Because snow is an important boundary forcing in the global climate system, much effort has been aimed at prediction and sources of predictability of snow cover variability and its climatic influences (*e.g.*, Yang 1996, Serreze *et al.* 1997, Corti *et al.* 2000, Bamzai 2003, Bojariu and Gimeno 2003, Sobolowski and Frei 2007). Snow physical properties such as albedo, thermal conductivity, emissivity and latent heat flux affect atmospheric circulations and render snow as a potential source of climate predictability on regional to hemispheric scales. Snow water equivalent (SWE), defined as the depth of water that would result if the mass of snow melted completely, is particularly useful for climate predictability as it contains regional information about previous climate anomalies (*e.g.*, temperature and precipitation) and can influence future climate on seasonal to longer time-scales. SWE is also essential to river and flood forecasting, and thus water resources planning and hazard mitigation (*e.g.*, droughts and floods), as it can be factored in with precipitation to determine the amount of runoff that might go into rivers and streams. Conversely, atmospheric circulations affect snowfall, snow mass and spring runoff predictability (*e.g.*, Sobolowski and Frei 2007). For example, snow anomalies respond to climate variability patterns such as the El Niño Southern Oscillation (ENSO), which is the largest single source of interannual variability in the tropics and is thus a major source of climate predictability with extratropical reach through its teleconnections (Groisman *et al.* 1994, Yang 1996, Ferranti and Molteni 1999, Martineu *et al.* 1999, Corti *et al.* 2000, Shaman and Tziperman 2005, Wu *et al.* 2012).

Here, we highlight key results on the potential and actual predictability of SWE historical forecasts (hindcasts) in the Fourth-Generation Coupled Climate Model (CanCM4), which is employed with CanCM3 to produce ensemble multi-seasonal forecasts by the Canadian Seasonal to Interannual Prediction System (CanSIPS; Merryfield *et al.* 2013) and contributes to the North American Multi-Model Ensemble (NMME; Kirtman *et al.* 2014). Specifically, we summarize sources and behaviour of potential and actual predictability of SWE hindcasts in CanCM4 at short and long time leads. Previously, the ability of CanSIPS to provide realistic initial conditions for snow cover forecasts was examined by Sospedra-Alfonso *et al.* (2015a).

### 2. Data and methods

CanCM4 was developed at the Canadian Centre for Climate Modelling and Analysis (CCCma). With CanCM3, it has been employed by CanSIPS to provide Environment Canada's operational seasonal forecasts since late 2011. CanCM4 is based on the Canadian Fourth-Generation Ocean Model (CanOM4), the Canadian Fourth-Generation Atmospheric General Circulation Model CanAM4 (also known as AGCM4), version 2.7 of the Canadian Land Surface Scheme (CLASS) and a sea ice cavitating fluid model. Details and relevant bibliography about these model components can be found in Merryfield *et al.* (2013).

In CanSIPS, each of the 10 CanCM4 forecast ensemble members is initialized from a separate assimilating run in which atmospheric winds, temperature, and humidity as well as sea surface temperature and sea ice concentration are constrained near observed values. Forecast initial conditions for the land component including snow cover are determined by the response of CLASS to forcing from model atmospheric fields constrained by 6-hourly reanalysis data. Thus, SWE initial conditions differ among

ensemble members. CanSIPS hindcasts are initialized at the beginning of each month during a multidecadal hindcast period and have a 12 month range.

We consider CanCM4 SWE hindcasts (1981–2010) in the Northern Hemisphere on the approximately  $2.8^\circ$  atmospheric/land surface model grid. We employ the following metrics:

- Potential predictability (PP) of monthly mean SWE in CanCM4 is examined by employing analysis of variance (ANOVA) (*e.g.*, von Storch and Swiers 1999) on the 10 ensemble members to estimate the fraction of interannual SWE variability that is potentially predictable. In this framework, the total interannual variability of SWE is partitioned into two components; (1) unpredictable chaotic fluctuations or noise, and (2) potentially predictable variability or “signal” variance associated with internal climate variability modes (*e.g.*, ENSO) and/or external forcing (*e.g.*, solar variability, explosive volcano eruptions, anthropogenic radiative forcing). The potential predictability of SWE is defined as the ratio of the signal to the total variance.

- Persistence of initial anomalies in CanCM4 SWE forecasts is given in terms of the temporal autocorrelation (AC) of predicted SWE anomalies, which is defined as the correlation between SWE forecast anomalies and the initial ensemble mean anomaly, averaged across the ensemble. The initial ensemble mean anomaly is employed instead of initial anomalies of individual ensemble members to account for uncertainty in the initial conditions of SWE anomalies, which results in a degradation of autocorrelation at the zero lead time.  $AC^2$  is a measure of the fraction of SWE variability that can be linearly attributed to the initial SWE anomalies, and can be compared with PP of SWE to assess the contribution of the memory of snowpack initial conditions to the potential predictability.

- ENSO influence on SWE is investigated by regressing CanCM4 forecast monthly mean SWE, surface temperature and precipitation on the monthly Niño 3.4 index (defined as the averaged sea surface temperature anomaly over the Pacific Ocean region  $5^\circ\text{S}$ - $5^\circ\text{N}$ ,  $120^\circ$ - $170^\circ\text{W}$ ).

- Actual skill in CanCM4 SWE forecasts is examined by computing the temporal anomaly correlation coefficient (ACC) between forecasts ensemble mean and a blend of 5 SWE observation-based products (Blended-5) developed by Mudryk *et al.* (2015), re-gridded to CanSIPS resolution. Blended-5 combines SWE from (1) the National Aeronautics and Space Administration (NASA) Modern-Era Retrospective analysis for Research and Application (MERRA; Rienecker *et al.* 2011), (2) the European Centre for Medium-Range Forecasts Interim Land Reanalysis (ERA-Interim/Land; Balsamo *et al.* 2013), (3) GlobSnow analysis, version 2, developed through the European Space Agency GlobSnow project and produced by the Finnish Meteorological Institute (Takala *et al.* 2011), (4) the Global Land Data Assimilation System Version 2 (GLDAS-2) product (Rodell *et al.* 2004), and (5) the Crocus snow scheme driven by ERA-Interim (Brun *et al.* 2013).

### 3. Summary of results and discussion

We identify two main sources of potential predictability and actual skill in CanCM4 SWE forecasts: (i) persistence of initial SWE anomalies, and (ii) SWE response to climate variations that are potentially predictable at longer time-scales, including ENSO.

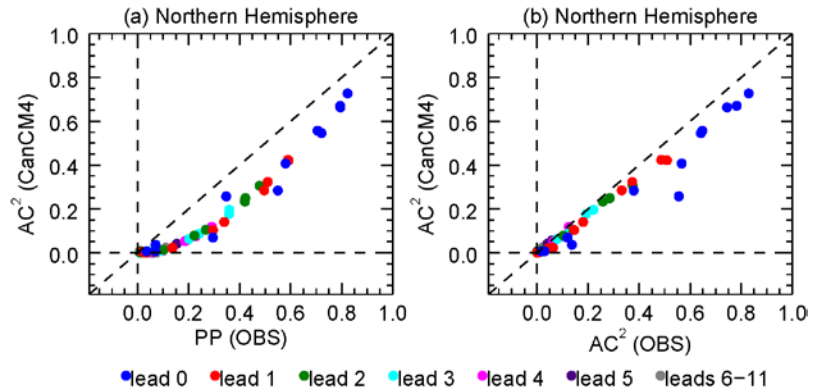


**Fig. 1** Scatter plots of Northern Hemisphere spatial means of  $AC^2$  for CanCM4 (vertical axis) vs (a) PP for CanCM4 (horizontal axis) and (b)  $AC^2$  for Blended-5 (horizontal axis) for each month and lead time in the forecast. Dots correspond to target months and colors denote lead times.

SWE depends cumulatively on previous snowfall and snowmelt events, therefore this “memory” in the form of anomaly persistence should contribute to PP. Spatial averages of PP and  $ACC^2$  over the Northern Hemisphere tend to be large and comparable to each other for short lead times (0-2 months) and much smaller for longer leads (over 4-month), with values that depend on the target month and initialization date (Fig. 1a). The short-range behaviour of PP is thus strongly determined by the persistence of initial SWE anomalies, particularly in regions of mature snowpack and/or initialization times in the core of the snow season. For example, for March-averaged SWE forecasts at 1-month lead (*i.e.*, initialized in February), which is prior to the start of the snowmelt and long after the snow onset in the mid-latitudes, high PP ( $> 0.8$ ) occurs in the higher latitudes ( $> 60^\circ N$ ), western Canada, and the Karakoram region (Fig. 2a). Geographic patterns of  $ACC^2$  (not shown) indicate that these regions are characterized by high SWE anomaly persistence.

PP determined by SWE anomaly persistence tends to decrease with lead time as the result of a relative increase in noise variance (due to ensemble dispersion), and with decreasing latitude and/or elevation due to a

relative decrease in signal variance associated with shorter snow seasons. For example, PP of March-averaged SWE at 11-month lead is insignificant ( $< 0.1$ ) in most of the Northern Hemisphere, with the exception of the Pacific Northwest, the southern Rocky Mountains and Karakoram (up to  $\approx 0.5$ ), and a few scattered regions in Asia and North America (Fig. 2b).

Spatially averaged  $ACC^2$  in CanCM4 SWE forecasts behaves similarly to that of the verifying observations (Fig. 1b). This suggests that CanCM4 should capitalize on SWE anomaly persistence as a source of actual skill, at least for short lead times. For example,  $ACC^2$  for March-averaged SWE forecasts at 1-month lead (Fig. 2c) has similar geographic patterns as PP (Fig. 2a), except in the Tibetan Plateau where PP is relatively high but  $ACC^2$  is  $< 0.1$ . As for PP,  $ACC^2$  tends to decay with lead time and is statistically insignificant at 11-month lead in most of the Northern Hemisphere, with the exception of the Pacific Northwest, the Karakoram region and a few scattered regions in Asia and North America (Fig. 2d).

The long-range behaviour of PP in CanCM4 (*e.g.*, Fig. 2b) is likely the result of SWE response to ENSO variability, combined with the ability of the forecasts to predict ENSO. Regression patterns of December and March-averaged SWE in forecasts initialized in the preceding April show that the regions where March-averaged SWE is potentially predictable (Fig. 2b) largely correspond with those where SWE anomalies associated with ENSO variability are statistically significant (Figs. 3a, b).

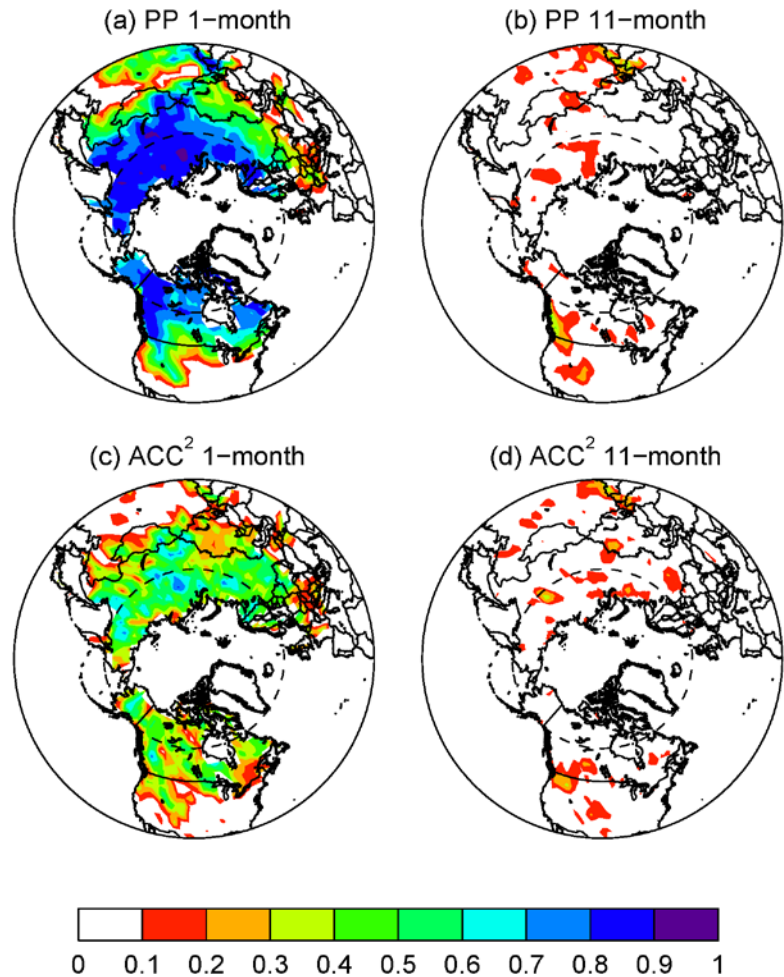


**Fig. 2** (top) PP and (bottom)  $ACC^2$  against Blended-5 of CanCM4 March-averaged SWE forecasts at (left) 1-month and (right) 11-month lead times indicating the time from forecast initial values.

SWE response to ENSO is likely driven by ENSO influences on temperature (T) and precipitation (P). Because of the SWE anomaly persistence discussed earlier, T and P influence on SWE is not limited to contemporary months but has contributions from previous months in the snow season (*e.g.*, Sospedra-Alfonso *et al.* 2015b). For example, regression patterns of December and March-averaged T and P corresponding to the forecasts initialized in April (Figs. 3c-f) reveal that negative anomalies of March-averaged SWE (Fig. 3b) in western Canada are likely the result of positive T and negative P anomalies already present in December (Fig. 3c, e) and November (not shown). This is likely the reason for the increased amplitude of ENSO-related SWE anomalies in March relative to December (Fig. 3a, b). Positive anomalies of December-averaged SWE (Fig. 3a) found in the southern U.S. Rocky Mountains are most likely due to negative T and positive P anomalies in December (Fig. 3c, e) and November (not shown). In the Karakoram, statistically significant positive anomalies of December-averaged SWE (Fig. 3a) are associated with positive P anomalies in December (Fig. 3e) and November (not shown), despite the slightly positive T anomalies in the region. These results support the idea that relatively high values of PP (Fig. 2b) and actual skill (Fig. 2d) for March-averaged SWE in the western North America and the Karakoram at 11-month lead is a signature of ENSO teleconnections.

#### 4. Concluding remarks

CanCM4 forecasts of SWE can display appreciable potential and actual skill depending on region, target month and initialization date. The behaviour of PP of SWE at short leads can be largely explained in terms of persistence of initial anomalies. Exploiting this source of PP as actual skill thus requires a reasonably accurate initialization of SWE, as occurs in CanSIPS (Sospedra-Alfonso *et al.* 2015a). The relative contribution of anomaly persistence to PP diminishes at longer lead times, implying that ability to predict future climate anomalies (*e.g.*, temperature and precipitation anomalies) contributes increasingly to PP as lead time increases. For long leads, PP of CanCM4 SWE forecasts appears to be mainly the result of SWE response to ENSO variability, combined with the ability of the forecasts to predict ENSO.

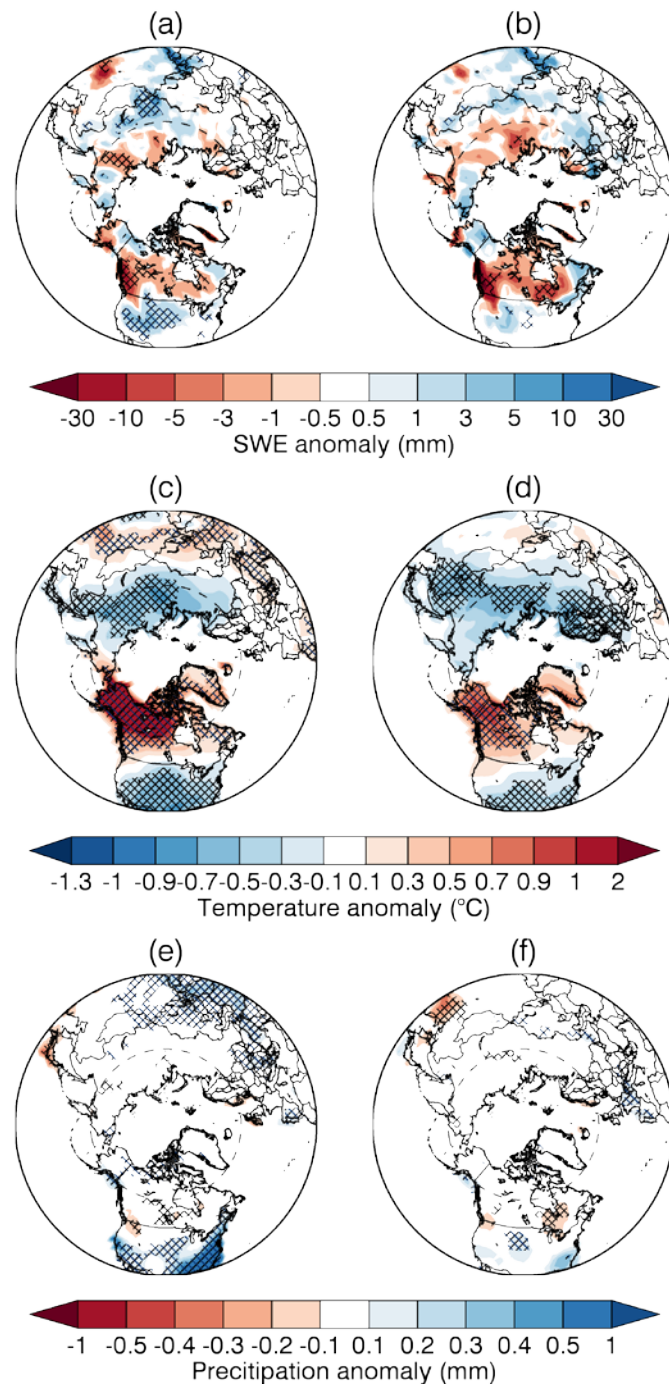


**Fig. 3** Regressions of CanCM4 predicted (left) December and (right) March averaged (a, b) SWE, (c, d) surface air temperature and (e, f) precipitation against CanCM4 predicted Niño 3.4 index for the forecasts initialized in April. Lead times are (left) 8 months and (right) 11 months. Cross hatched regions correspond to correlations  $>0.3$ .

For long leads, PP of CanCM4 SWE forecasts appears to be mainly the result of SWE response to ENSO variability, combined with the ability of the forecasts to predict ENSO.

*Disclaimer.* This note complements a detailed work on potential and actual predictability of snow in CanSIPS submitted for publication in the Journal of Hydrometeorology.

## References

- Balsamo, G., and Coauthors, 2013: ERA-Interim/Land: a global land water resources dataset. *Hydrology and Earth System Sciences Discussions*, **10**, 14,705–14,745.
- Bamzai, A. S., 2003: Relationship of snow cover variability and Arctic oscillation index on a hierarchy of time scales. *International Journal of Climatology*, **23**, 131–142.
- Bojariu, R., and L. Gimeno, 2003: The role of snow cover fluctuations in multiannual NAO persistence. *Geophysical Research Letters*, **30**, 1156.
- Brun, E., V. Vionnet, A. Boone, B. Decharme, Y. Peings, R. Valette, F. Karbou, and S. Morin, 2013: Simulation of northern Eurasian local snow depth, mass, and density using a detailed snowpack model and meteorological reanalyses. *Journal of Hydrometeorology*, **14**, 203–219.
- Corti, S., F. Molteni, and Č. Branković, 2000: Predictability of snow-depth anomalies over Eurasia and associated circulation patterns. *Quarterly Journal of Royal Meteorological Society*, **126**, 241–262.
- Ferranti, L., and F. Molteni, 1999: Ensemble simulations of eurasian snow-depth anomalies and their influence on the summer asian monsoon. *Quarterly Journal of the Royal Meteorological Society*, **125**, 2597–2610.
- Groisman, P. Y., T. R. Karl, and R. W. Knight, 1994: Changes of snow cover, temperature, and radiative heat balance over the northern hemisphere. *Journal of Climate*, **7**, 1633–1656.
- Kirtman, B., and Coauthors, 2014: The North American Multimodel Ensemble: Phase-1 seasonal-to-interannual prediction; Phase-2 toward developing intraseasonal prediction. *Bulletin of the American Meteorological Society*, **95**, 585–601.
- Martineu, C., J.-Y. Caneill, and R. Sadourny, 1999: Potential predictability of European winters from the analysis of seasonal simulations with an AGCM. *Journal of Climate*, **12**, 3033–3061.
- Merryfield, W. J., W.-S. Lee, G. J. Boer, V. V. Kharin, J. F. Scinocca, G. M. Flato, R. S. Ajayamohan, and J. C. Fyfe, 2013: The Canadian Seasonal to Interannual Prediction System. Part I: Models and Initialization. *Monthly Weather Review*, **141**, 2910–2945.
- Mudryk, L. R., C. Derksen, P. J. Kushner, and R. Brown, 2015: Characterization of Northern Hemisphere snow water equivalent datasets, 1981-2010. *Journal of Climate*, **28**, 8037–8051.
- Rienecker, M. M., and Coauthors, 2011: MERRA - NASA's modern-era retrospective analysis for research and applications. *Journal of Climate*, **24**, 3624–3648.
- Rodell, M., and Coauthors, 2004: The Global Land Data Assimilation System. *Bulletin of the American Meteorological Society*, **85**, 381–394.
- Serreze, M. C., F. Carse, R. G. Barry, and J. C. Rogers, 1997: Icelandic low cyclone activity: Climatological features, linkages with the NAO, and relationships with recent changes in the Northern Hemispheric circulation. *Journal of Climate*, **10**, 453–464.
- Shaman, J., and E. Tziperman, 2005: The effect of ENSO on Tibetan Plateau snow depth: A stationary wave teleconnection mechanism and implications for the south Asian Monsoons. *Journal of Climate*, **18**, 2067–2079.
- Sobolowski, S., and A. Frei, 2007: Lagged relationships between North American snow mass and atmospheric teleconnections indices. *International Journal of Climatology*, **27**, 221–231.
- Sospedra-Alfonso, R., L. Mudryk, W. J. Merryfield, and C. Derksen, 2015a: Representation of snow in the Canadian Seasonal to Interannual Prediction System: Part I. Initialization. *Journal of Hydrometeorology*. doi: 10.1175/JHM-D14-0223.1
- Sospedra-Alfonso, R., J. R. Melton, and W. J. Merryfield, 2015b: Effects of temperature and precipitation on snowpack variability in the Central Rocky Mountains as a function of elevation. *Geophysical Research Letters*, **42**, 4429–4438.

- Takala, M., K. Luojus, J. Pulliainen, C. Derksen, J. Lemmetyinen, J.-P. Karna, J. Koskinen, and B. Bojkov, 2011: Estimating northern hemisphere snow water equivalent for climate research through assimilation of space-borne radiometer data and ground-based measurements. *Remote Sensing of Environment*, **115**, 3517–3529.
- von Storch, H., and F. W. Zwiers, 1999: Statistical Analysis in Climate Research. *Cambridge University Press*, 484 pp.
- Wu, Z., J. Li, Z. Jiang, and T. Ma, 2012: Modulation of the Tibetan Plateau snow cover on the ENSO teleconnections: From the east Asian summer monsoon perspective. *Journal of Climate*, **25**, 2481–2489.
- Yang, S., 1996: ENSO-snow-monsoon associations and seasonal-interannual predictions. *International Journal of Climatology*, **16**, 125–134.